FEBS Letters 581 (2007) 3356–3362

Reticulon-like proteins in *Arabidopsis thaliana*: Structural organization and ER localization

Hugues Nziengui[1], Karim Bouhidel, David Pillon, Christophe Der, Francis Marty, Benoît Schoefs*

UMR Plante-Microbe-Environnement, INRA 1088/CNRS 5184/Université de Bourgogne, BP 47870, Université de Bourgogne, F-21078 Dijon Cedex, France

Received 8 May 2007; revised 12 June 2007; accepted 12 June 2007

Available online 21 June 2007

Edited by Ulf-Ingo Flügge

Abstract **Reticulons are proteins that have been found predominantly associated with the endoplasmic reticulum in yeast and mammalian cells. While their functions are still poorly understood, recent findings suggest that they participate in the shaping of the tubular endoplamic reticulum (ER). Although reticulon-like proteins have been identified in plants, very little is known about their cellular localization and functions. Here, we characterized the reticulon-like protein family of *Arabidopsis thaliana*. Three subfamilies can be distinguished on the basis of structural organization and sequence homology. We investigated the subcellular localization of two members of the largest subfamily, i.e. AtRTNLB2 and AtRTNLB4, using fluorescent protein tags. The results demonstrate for the first time that plant reticulon-like proteins are associated with the ER. Both AtRTNLB proteins are located in the tubular ER but AtRTNLB4 is also found in the lamellar ER cisternae, and in ER tubules in close association with the chloroplasts. Similarity in protein structure and subcellular localization between AtRTNLB2 and mammalian reticulons suggests that they could assume similar basic functions inside the cell.**

Keywords: Chloroplast; Endoplasmic reticulum; RTLNB; Reticulon; *Arabidopsis thaliana*

1. Introduction

Reticulons (RTNs) were first described as integral membrane proteins of the endoplasmic reticulum (ER) in mammalian neurons [1,2]. RTN genes have now been identified in all eukaryotic genomes studied [3]. RTNs share a 200-amino-acid residue region of sequence similarity at the C-terminus; the reticulon homology domain (RHD), which is responsible for the association to the ER membrane. This region is composed of two hydrophobic regions spaced by an ~60-amino-acid loop (Fig. 1) [4]. RTN membrane topology is thought to be primarily determined by the number of membrane-spanning segments lying within the two hydrophobic regions as illustrated in Fig. 1 [5]. RTNs are predominantly found in the tubular ER where they might act as membrane stabilizers [6]. Mammalian RTNs have been shown to be involved in endocytosis [7], intracellular transport [8,9], and it has been suggested that they play a role in apoptosis, axonal growth and regeneration [5]. Reticulon homologs from nonchordate taxa have been classified into six reticulon-like protein subfamilies (RTNL), including the plant subfamily of RTNLs named RTNLB [3]. Very little is known about the subcellular localization and functions of RTNLBs. Marmagne et al. [10] have identified two RTNLBs from *Arabidopsis thaliana* (AtRTNLB1 and AtRTNLB6) in plasma membrane (PM)-enriched fractions. Hwang and Gelvin [11] have shown that AtRTNLB1 (named VirB2-interacting protein (BTI1)), AtRTNLB2/BTI2 and AtRTNLB4/BTI3 influence the susceptibility to *Agrobacterium tumefaciens*-mediated transformation and interact with VirB2, the major component of the *Agrobacterium* T-pilus. In the same study, the three AtRTLNBs, fused to green fluorescent protein (GFP), have been localized to the periphery of root cells but no association with a specific organelle has been characterized. So far, and in contrast to mammalian RTNs, reticulon-like proteins from plants have not been reported as being localized to the ER.

In the present study, we identified 21 sequences encoding RHD-containing proteins from the *A. thaliana* genome in silico. The overall organization of most AtRTNLBs is reminiscent of those of mammalian RTNs, leading us to suggest that they might share similar functions. Differences within or outside the RHD may however indicate functional differences between members of the AtRTNLB family. We also investigated the subcellular localization of AtRTNLB2 and AtRTLNB4, and observed two different association patterns with ER subcompartments.

2. Materials and methods

2.1. Plant materials and growth conditions

A. thaliana plants (ecotype Columbia) were grown on a 1:1 mixture of soil and compost in a growth chamber under controlled conditions (70% relative humidity, 16 h of light with a photon flux density of

*Corresponding author. Fax: +33 3 80 39 50 66.
E-mail address: benoit.schoefs@u-bourgogne.fr (B. Schoefs).

[1]Present address: Institut für Biologie II, Universität Freiburg, Schänzlestrasse 11, D-79104 Freiburg, Germany.

Abbreviations: At3βHSD/D2, *A. thaliana* 3β-hydroxysteroid dehydrogenase/C-4 decarboxylase 2; BTI, VirB2-interacting protein; CaMV, cauliflower mosaic virus; CTR, C-terminal region; ER, endoplasmic reticulum; EST, expressed sequence tag; GFP, green fluorescent protein; HR, hydrophobic region; NTR, N-terminal region; PM, plasma membrane; RHD, reticulon homology domain; RTN, reticulon; RTNL, reticulon-like protein; RTNLB, reticulon-like protein B; MSS, membrane-spanning segment; YFP, yellow fluorescent protein

0014-5793/$32.00
doi:10.1016/j.febslet.2007.06.032

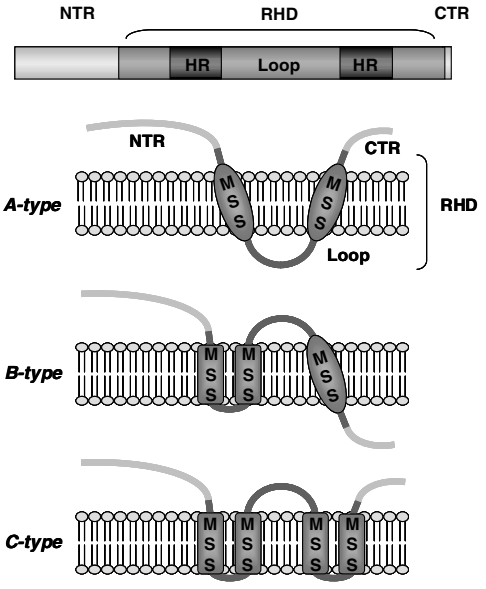

Fig. 1. Structural organization of reticulons and putative membrane topologies. The precise topology of reticulons is not known and the illustrated topologies are based almost exclusively on predictions by computer programs. The N- and C-terminal regions (NTR, CTR) are found on one side or on either of the membrane, depending on the number of membrane-spanning segments (MSS) within each hydrophobic region (HR) of the reticulon homology domain (RHD).

50 μmol m^{-2} s^{-1} at 25 °C and 8 h of dark at 20 °C). Lighting was provided by a combination of fluorescent tubes (Mazda TF36WSA/79) and incandescent lamps (OSRAM 40 W, 230 V, 4 K).

2.2. Bioinformatics analysis

Search for putative RTNLB genes, cDNAs and expressed sequence tag (ESTs) from *A. thaliana* were conducted in TAIR (http://www.arabidopsis.org/) and in Aramemnon databases (http://aramemnon.botanik.uni-koeln.de/). The RHD search was performed with Pfam program (http://pfam.wustl.edu/hmmsearch.shtml). Prediction of membrane-spanning segment (MSS) was made with five different methods (DAS, SOSUI, TMHMM, HMMTOP and TopPred) on ExPASy Proteomics server (http://www.expasy.org/tools/). The number of predicted MSSs varied depending on the method used, so we took into account only MSSs that were identified with at least three different methods. The identification of protein motifs was made with ELM software (http://elm.eu.org/). Sequence alignments were performed by using CLUSTAL W v.1.83 [12] under the following parameter settings: Gonnet 250 as protein weight matrix, 10 and 0.2 as gap opening and gap extension penalties for pairwise and multiple alignments. Aligned sequences were then edited by BioEdit software v.7.0.5 (Carlsbad, CA). The molecular phylogenetic tree was drawn using MEGA version 3.1 [13] as follows: the amino acid sequences were first aligned by CLUSTAL W, then subjected to neighbor-joining tree construction using Poisson correction distance with bootstrap test (500 replicates).

2.3. Plant vector construction

The cDNA clones corresponding to AtRTNLB2 (At4g11220) and AtRTNLB4 (At5g41600) proteins were obtained from RIKEN BioResource Center (http://www.brc.riken.jp/inf/en/). Coding sequences were PCR-amplified using primer pairs GWB2-F (5′-CAATGGCGGATGAACATAAGCATG-3′) and GWB2-R (5′-AATCCTTCTTCTTGTCTTTCAACGG-3′) for AtRTNLB2, GWB4-F (5′-CAACAAAAATGGTGGA-AGACCAC-3′) and GWB4-R (5′-AATCCTTCTTCTTGTTCAGAGC-3) for AtRTNLB4. PCR products were cloned into Gateway entry vector pDONR221 (Invitrogen, Cergy-Pontoise, France), then subcloned into plant transformation vectors pMDC83 [14] and pMDC83Y (a yellow fluorescent protein (YFP)-encoding pMDC83 vector), giving plasmids pRTNLB2:GFP and pRTNLB4:YFP, respectively.

2.4. Plant transformation

The pRTNLB2:GFP and pRTNLB4:YFP plasmids were introduced into *A. tumefaciens* strain C58C1 according to An et al. [15], and the resulting agrobacteria were then used for floral infiltration of *A. thaliana* plants [16]. Infiltrated seeds were surface sterilized and plated onto MS-hygromycin B (20 μg/ml) solid medium. Plates were incubated in the dark at 4 °C for 2 days, exposed to light for 6 h and put back to darkness for 4 days at 22 °C. Hygromycin-resistant seedlings with long hypocotyls were then transferred into soil.

2.5. Protoplast preparation

Protoplasts were prepared from rosette leaves of 3–4-week-old transgenic *A. thaliana* plants as described by Bauer et al. [17].

2.6. Confocal microscopy

Before observation, protoplasts and pieces of leaves were mounted in protoplast medium [17] and water, respectively. When needed, a few drops of the FM-dye FM4-64 (Molecular Probes, Leiden, The Netherlands) at the concentration of 10^{-7} M were added into the mounting medium. Fluorescence observations were conducted with a Leica TCS-SP2-AOBS confocal microscope (Leica Microsystems, Wetzlar, Germany). Excitation wavelengths and emission filters were 488 nm/band-pass 506–538 nm for GFP, 488 nm/band-pass 664–696 nm for FM4-64 and chlorophyll, and 514 nm/band-pass 539–595 nm for YFP. Images were processed using Photoshop 6.0 (Adobe Systems, San Jose, CA).

3. Results and discussion

3.1. The RTNLB protein family in A. thaliana

In order to identify AtRTNLB genes in the *A. thaliana* genome, we blasted the RHD sequence against the TAIR and Aramemnon databases. The search successfully identified 21 genes (Table 1). Fifteen of the 21 gene products are named as AtRTNLB1 to AtRTNLB15 in Aramemnon database. According to this nomenclature, we suggest to name the six other proteins as AtRTNLB16 to AtRTNLB21. At least, one full-length cDNA from TAIR database was associated with all but four AtRTNLBs listed in Table 1. For convenience, we have chosen to report a single splice variant for each AtRTNLB. It is however likely that, similarly to animal RTN genes, a single AtRTNLB gene can give rise to multiple isoforms originating from alternative splicing and/or the use of alternative promoters [3]. Gene expression markers such as ESTs and partial or full-length cDNAs have been found for all but the AtRTNLB7 and AtRTNLB14 genes. The numbers of ESTs indicate that AtRTNLB genes behave differently in terms of expression level and/or range of cell specificity.

Previously identified AtRTNLBs (1–15) display the canonical reticulon organization with (i) a short N-terminal region (NTR: 13–88 aa), and (ii) a C-terminal RHD (Table 1 and [4]). Most of the new RHD-containing proteins (AtRTNLB16–21) show long N-terminal regions (NTR) and/or C-terminal regions (CTR), up to 383 and 85 aa, respectively (Table 1). In Pfam database, less than 1% of all metazoan RHD-protein entries (2/246) displays a CTR. The percentage reaches 11% for RTNLBs (6/55) and 100% for fungi RTN-like proteins (10/10). The functional significance of such differences remains to be elucidated.

The RHD of AtRTNLBs is fairly conserved in length (173–188 aa, Table 1) despite sequence divergence (12–89% identity in pairwise alignments). Asp3 and Trp7 are the only strictly conserved residues among the 21 analyzed RHD sequences (Fig. 2). We used the DAS, SOSUI, TMHMM, HMMTOP, and TopPred methods to characterize the topology of

Table 1
The AtRTNLB protein family

Name	Locus	Length[a]	NTR[a]	RHD[a]	CTR[a]	MSS[b]	Loop[a,c]	EST[d]	K(X)KXX[e]
AtRTNLB1[f]	At4g23630	275	88	184	3	4	56	416	+
AtRTNLB2[g]	At4g11220	271	84	184	3	4	56	84	+
AtRTNLB3	At1g64090	255	63	188	4	4	56	77	+
AtRTNLB4[h]	At5g41600	257	67	188	2	4	58	47	+
AtRTNLB5	At2g46170	255	67	184	4	4	60	22	+
AtRTNLB6	At3g61560	253	67	184	2	3	52	8	+
AtRTNLB7	At4g01230[i]	242	67	174	1	3	51	0	–
AtRTNLB8[j]	At3g10260	247	60	184	3	2	56	45	+
AtRTNLB9	At3g18260	225	38	184	3	3	52	2	+
AtRTNLB10	At2g15280	201	13	183	5	3	60	9	+
AtRTNLB11	At3g19460	200	21	176	3	3	60	15	+
AtRTNLB12	At3g54120	203	23	178	2	3	55	33	+
AtRTNLB13	At2g23640[k]	206	15	178	13	3	52	0	+
AtRTNLB14	At1g68230[i]	215	30	178	7	3	47	0	–
AtRTNLB15[l]	At2g01240[k]	179	NI[m]	179	0	3	57	0	–
AtRTNLB16[n,o]	At3g10915	226	40	186	0	3	56	25	+
AtRTNLB17[n]	At2g20590	431	167	188	76	4 (1)	61	5	–
AtRTNLB18[n]	At4g28430	457	194	182	81	4 (1)	62	20	+
AtRTNLB19[n,p]	At2g26260	564	383	181	0	4 (1)	59	15	+
AtRTNLB20[n]	At2g43420	561	378	179	4	3	61	33	–
AtRTNLB21[n]	At5g58000[q]	487	229	173	85	4 (1)	61	4	+

[a]Length in amino acids.
[b]MSS: Number of membrane-spanning segments. The number of MSSs outside the RHD is indicated in parenthesis.
[c]Mean value of lengths predicted by 5 different softwares.
[d]EST number from TAIR database.
[e]C-terminal di-lysine sorting signal.
[f]Named BTI1 in Ref. [11].
[g]Named BTI2 in Ref. [11].
[h]Named BTI3 in Ref. [11].
[i]No cDNA has been found for the locus.
[j]Name given by Ortle et al. [3].
[k]A partial cDNA has been found for the locus.
[l]A new splice variant with a better-fitting RHD.
[m]The NTR has Not been Identified.
[n]New name.
[o]Splice variant number 2 in TAIR database.
[p]Named At3βHSD/D2 in Ref. [20].
[q]The locus encompasses 2 transcription units. We have retained the 5′ unit, which encodes an RHD-containing protein.

AtRTNLBs. A consensus emerged from the prediction analyses although there was some variation in the exact number and position of predicted membrane-spanning segments. The five methods detected two hydrophobic regions spaced by a ~60-amino-acid hydrophilic loop within the RHD (Table 1 and Fig. 2). The prediction methods also mostly agreed on the fact that the hydrophobic region on the N-terminal side of the RHD is long enough to include two MSSs with a short linker, but did not always agree on the exact number of MSSs within the second hydrophobic region. An additional MSS was also found in the CTR of AtRTNLB17, AtRTNLB18 and AtRTNLB21 and in the NTR of AtRTNLB19. So, all AtRTNLBs but one would display the B-type or C-type topology as illustrated in Fig. 1. Some of the methods that we used also specified MSS orientation but gave conflicting predictions. Future investigations such as epitope localization or sided digestion with proteases will be required to establish a definitive topology for each AtRTNLB.

We conducted a computer search for other peptide sequences that could link AtRTNLBs to the ER. All AtRTNLB NTRs lack an ER signal peptide, suggesting that translocation into the ER, if any, is directed by internal signals (e.g., transmembrane domains). However, the di-lysine signal K(X)KXX, an ER retention and retrieval signal of various membrane-bound protein in animal and plant cells [18,19], was found at the C-terminus of 16 AtRTNLBs (Table 1).

Protein domain search within terminal regions detected a 3β-hydroxysteroid dehydrogenase/isomerase domain in AtRTNLB19 (also named At3βHSD/D2 in [20]) and AtRTNLB20 NTRs. A 3β-hydroxysteroid dehydrogenase/C-4 decarboxylase activity has been recently proven in vitro for a truncated version of AtRTNLB19/At3βHSD/D2 (i.e. without the RHD) and for the At1g47290 gene product, an RHD-less protein showing 83% identity to AtRTNLB19 [20]. Sequence comparison of both genes indicates that At1g47290 ancestor probably had an RHD-coding sequence.

To determine the evolutionary relationships among *A. thaliana* RTNLBs, a phylogenetic analysis was performed using the RHD. The amino-acid sequences were aligned and analyzed by the neighbor-joining method to infer a phylogenetic tree. The two *Saccharomyces cerevisiae* RHD sequences were used as the outgroup according to classical taxonomy. The phylogram indicates the existence of three well-supported clusters, designated as I, II and III (Fig. 3). In cluster I are found AtRTNLBs with short NTR and no CTR, in cluster II the two AtRTNLBs with long NTR, and in cluster III the three AtRTNLBs with long NTR and CTR. Within cluster I, phylogenetic relationships are not clearly defined because of internal

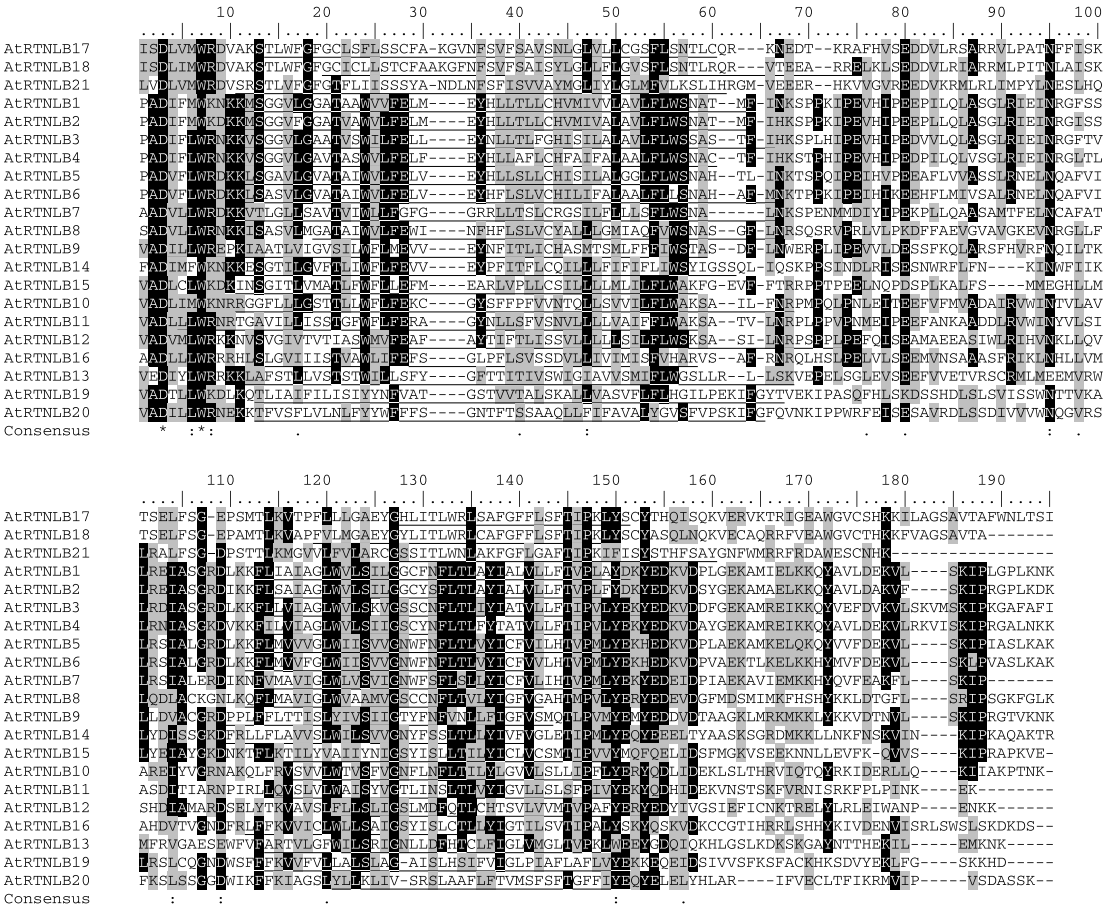

Fig. 2. Protein sequence alignment of *A. thaliana* reticulon homology domains. The alignment was performed using CLUSTAL W. In the alignment, dashes are gaps, identical and similar amino acids are highlighted with black and grey boxes, respectively. In the consensus sequence, asterisks (*) show identical amino acids in all sequences of the alignment, (:) and (.) indicate conservative and semi-conservative substitutions. Regions with stretches of hydrophobic amino-acid residues are underlined.

nodes without strong bootstrap support. We retrieved from Pfam database all RHD sequences from RTNLBs with long NTR alone (Os-Q7Y0G4, Os-Q69IL0) and long NTR and CTR (Os-Q6K5U2, Mt-Q1RY25), and included them into our phylogenetic analysis (Fig. 3). The supplemental sequences add, as expected, new branches in clusters II and III, respectively. In a final analysis, all non-*Arabidopsis* sequences from short NTR-proteins (18 Pfam entries) were also included and gave a similar tree topology with new branches in cluster I. The corresponding tree is not presented here for clarity only. In conclusion, the phylogenetic analysis strongly supports the subdivision of the *A. thaliana* reticulon-like protein family, and, to a larger extent, the plant reticulon-like protein family, into three subfamilies on the basis of structural organization and RHD sequence homology.

3.2. Subcellular localization of AtRTNLB2 and AtRTNLB4 proteins

Until now, the ER association for plant reticulon-like proteins has been inferred from their RHD-coding capacity. To challenge such an hypothesis, we investigated the subcellular localization of two AtRTNLBs from cluster I. The AtRTNLB2 and AtRTNLB4 coding sequences were placed under the control of the constitutive CaMV 35S promoter and fused in frame with GFP and YFP coding sequences, respectively. The resulting fusion genes were then introduced into *A. thaliana* genome via *A. tumefaciens*-mediated transformation. No distinctive phenotypes were observed when transgenic plants were grown in soil, indicating that the constitutive expression of the reticulon-like proteins did not affect the development and physiology of the transformed plants (data not shown).

Using fluorescence confocal microscopy, we monitored epidermal and mesophyll transformed cells from young leaves (Figs. 4 and 5). Grazing optical sections of epidermal cells expressing either AtRTNLB2:GFP or AtRTNLB4:YFP displayed a fluorescent polygonal network (Fig. 4A and B). This very distinctive network was identified as tubular ER based on previously published reports [21–23].

The lipophilic styryl dye FM4-64 was used to visualize the plasma membrane of transformed cells after short incubation times (Fig. 4C-F). FM4-64 accumulated in a clear and sharp continuous line at the periphery of epidermal cells. In confocal cross sections through the epidermis, FM4-64 labelling could be seen as two separate lines from two adjacent cells, leaving the cell wall space unstained (Fig. 4C and E). As shown in Fig. 4D and F, the labelling patterns for the PM marker FM4-64 and for the chimeric proteins AtRTNLB2:GFP and AtRTNLB4:YFP were distinct, indicating that none of these two reticulon-like proteins accumulates in the plasma membrane.

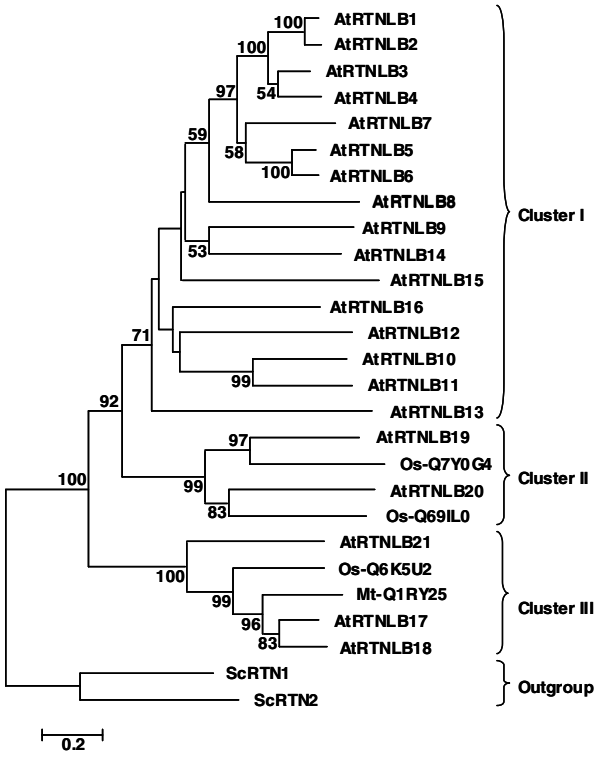

Fig. 3. Phylogenetic relationships of RTNLBs. The compiled RHD sequences were aligned using the ClustalW software. The tree was inferred by the neighbour-joining method and drawn using the MEGA3 software. *Saccharomyces cerevisiae* RHDs (ScRTN1 and ScRTN2) were used as the outgroup. Results of the bootstrap test (500 repetitions) are indicated when higher than 50. Rice and barrel medic RHDs are, respectively, defined as Os- or Mt- followed by the Uniprot accession number of the corresponding RTNLB.

Both AtRTNLBs were reported to influence the susceptibility to *A. tumefaciens*-mediated transformation and to interact with VirB2, the major component of the *A. tumefaciens* T-pilus [11]. The T-pilus is a filamentous appendage that is essential for T-DNA transfer and virulence but whose interaction with the plant cell membrane is not known. Our observation indicates that AtRTNLB2 and AtRTNLB4 are not PM-resident proteins. Thus, the direct interaction with the bacterial pilin could be explained if the T-pilus penetrates the plasma membrane. Alternatively, the interaction could occur at the cell surface if AtRTNLBs shuttle between the cortical ER and the PM in contact zones. The resolution of our confocal images does not allow us to rule out the shuttling hypothesis.

We then examined the overall distribution of the fluorescent labelling in mesophyll cells and mesophyll cell-derived protoplasts (Fig. 5). AtRTNLB4:YFP did not solely labelled ER tubules from the polygonal network but also numerous tubules tightly encircling the chloroplasts and connected to the polygonal network (Fig. 5A and B). The association with chloroplast-encircling tubules was less obvious for AtRTNLB2:GFP (Fig. 5E and F). Close associations between ER and chloroplasts were previously visualized in plant cells by electron microscopy [24,25] and confocal microscopy [26,27]. It has been suggested that appositional contacts between ER and the chloroplast envelope may mediate the rapid transfer of lipids [28]. Strong attracting forces have been shown to occur at the membrane contact sites and could involve protein-protein interactions [27]. Whether ER-anchored reticulon-like proteins take part into this process remains to be determined.

AtRNLB4:YFP was also found associated with lamellar ER cisternae in a population of small protoplasts (Fig. 5C). The more intense fluorescence signal at the lamellar cisternae periphery suggests that AtRTNLB4 is embedded in the ER membrane. AtRTNLB2:GFP was never found to label lamellar cisternae, but was found to highlight cable-like structures connected to tubular ER (Fig. 5F). Boevink et al. [22] have shown that the ER network overlays a network of actin filaments. Our cable-like structures likely correspond to bundled ER tubules in connection with underlying bundles of actin filaments.

Finally, AtRTNLB4:YFP was also observed in small bodies occurring at the vertices of the tubular network (Fig. 5B). By reducing the intensity of the laser beam, such bodies were resolved into doughnut-shaped structures (Fig. 5D). Similar structures have been previously observed in tobacco cells and

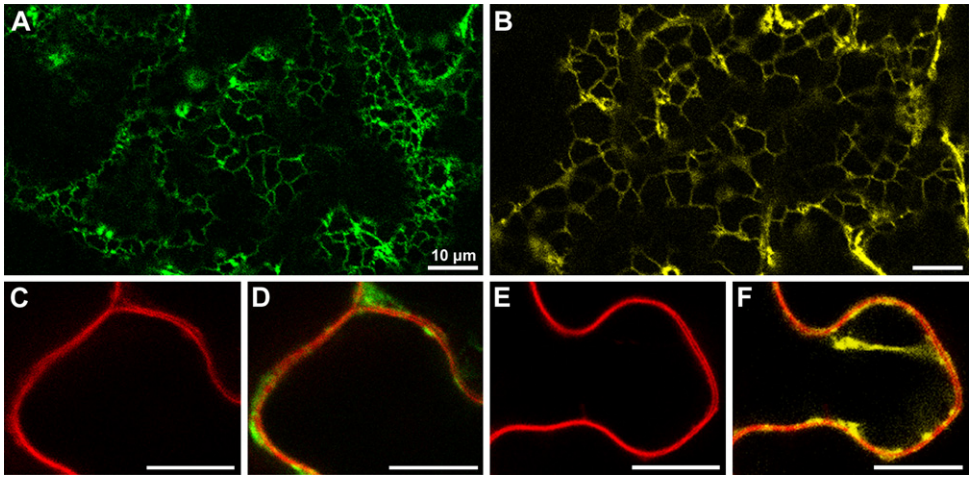

Fig. 4. ER localization of AtRTNLB2:GFP and AtRTNLB4:YFP proteins in epidermal cells. (A,B) Periclinal confocal sections of the cell cortex showing ER tubules labelled with AtRTNLB2:GFP and AtRTNLB4:YFP, respectively. (C–F) Periclinal confocal sections through the middle of the epidermal cell layer showing adjacent plasma membranes (FM4-64 red fluorescence) and cortically-localized AtRTNLB2:GFP in (D) or AtRTNLB4:YFP in (F). Scale bars = 10 µm.

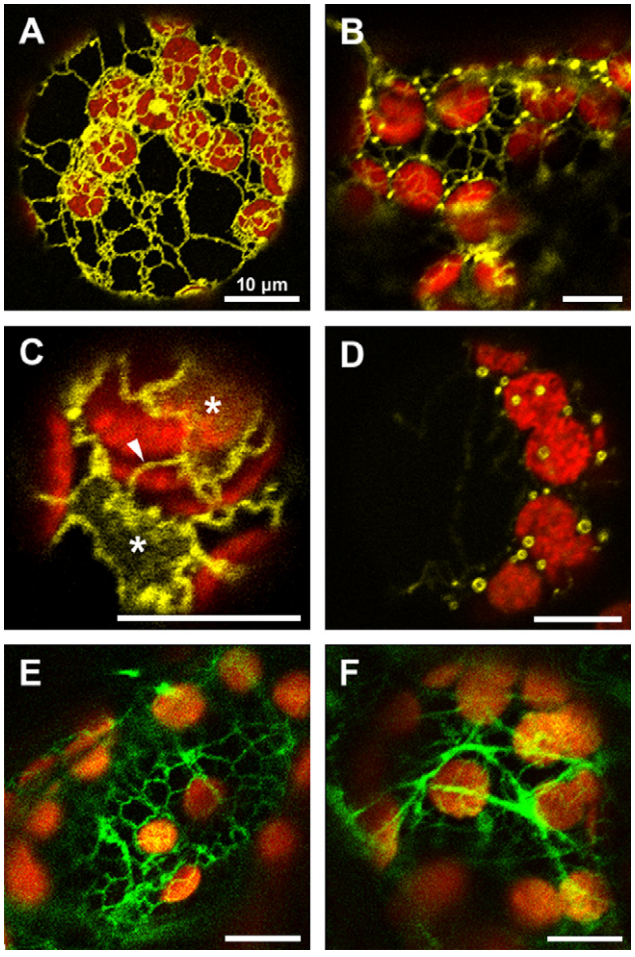

Fig. 5. Distinctive intracellular localizations for AtRTNLB2:GFP and AtRTNLB4:YFP proteins in mesophyll cell-derived protoplasts (A, C, D) and mesophyll cells (B, E, F). (A–D) Mergers of AtRTNLB4:YFP and chlorophyll fluorescence images showing that the fusion protein labels ER tubules in close association with chloroplasts in (A) and (B), lamellar ER cisternae (asterisks) in connection with ER tubules (white arrowhead) in (C), and small bodies in the vicinity of the chloroplasts in (B) and (D). (E,F) Mergers of AtRTNLB2:GFP and chlorophyll fluorescence images highlighting the polygonal ER network in (E) and cable-like structures in (F). Scale bars = 10 μm.

identified as Golgi stacks [22]. Further experiments will be required to determine whether the native AtRTNLB4 is also targeted to both ER and Golgi apparatus and plays a role in membrane trafficking in the early secretory pathway as it has been demonstrated for human RTN3 [9].

4. Conclusions

The reticulon-like protein family from *A. thaliana* comprises 21 members (AtRTNLB1–21), most of which displaying the canonical reticulon organization with a C-terminal RHD composed of transmembrane regions linked by a hydrophilic loop. Here we show, that similarly to animal reticulons, plant reticulon-like proteins (i.e. AtRTNLB2 and 4) are associated with the ER. However, the distribution patterns throughout the ER continuum differ. Indeed, if both proteins have been found associated with the tubular cisternae, only AtRTNLB4 labels lamellar cisternae and tubules in close contact with chloroplasts. A recent publication describes the contribution of human and yeast reticulons to the formation and maintenance of ER tubules [6]. The fact that AtRTNLB2 is specifically located in the tubular subcompartments of the ER suggests that it could play a similar role in *A. thaliana* cells. AtRTNLB4 location in the lamellar cisternae may link the reticulons to functions different from their role in ER tubule formation.

Acknowledgements: H.N. gratefully acknowledges the support of postdoctoral fellowship No. HCP13 from the Conseil Régional de Bourgogne. This work was also supported by grants from the French Ministère de l'Education Nationale, de l'Enseignement Supérieur et de la Recherche, INRA and CNRS. We thank the RIKEN BioResource Center for the gift of cDNA clones. We are grateful to Dr. C. Humbert for his help with the confocal microscope.

References

[1] Roebroek, A.J., van de Ven, W.J., Van Bokhoven, A., Broers, J.L. and Ramaekers, F.C. (1993) Cloning and expression of alternative transcripts of a novel neuroendocrine-specific gene and identification of its 135-kDa translational product. J. Biol. Chem. 268, 13439–13447.
[2] van de Velde, H.J., Senden, N.H., Roskams, T.A., Broers, J.L., Ramaekers, F.C., Roebroek, A.J. and Van de Ven, W.J. (1994) NSP-encoded reticulons are neuroendocrine markers of a novel category in human lung cancer diagnosis. Cancer Res. 54, 4769–4776.
[3] Oertle, T., Klinger, M., Stuermer, C.A. and Schwab, M.E. (2003) A reticular rhapsody: phylogenic evolution and nomenclature of the RTN/Nogo gene family. FASEB J. 17, 1238–1247.
[4] Oertle, T. and Schwab, M.E. (2003) Nogo and its partners. Trends Cell Biol. 13, 187–194.
[5] Yan, R., Shi, Q., Hu, X. and Zhou, X. (2006) Reticulon proteins: emerging players in neurodegenerative diseases. Cell Mol. Life Sci. 63, 877–889.
[6] Voeltz, G.K., Prinz, W.A., Shibata, Y., Rist, J.M. and Rapoport, T.A. (2006). A class of membrane proteins shaping the tubular endoplasmic reticulum. Cell 124, 573–586.
[7] Iwahashi, J. et al. (2002) *Caenorhabditis elegans* reticulon interacts with RME-1 during embryogenesis. Biochem. Biophys. Res. Commun. 293, 698–704.
[8] Steiner, P., Kulangara, K., Sarria, J.C., Glauser, L., Regazzi, R. and Hirling, H. (2004) Reticulon 1-C/neuroendocrine-specific protein-C interacts with SNARE proteins. J. Neurochem. 89, 569–580.
[9] Wakana, Y. et al. (2005) Reticulon 3 is involved in membrane trafficking between the endoplasmic reticulum and Golgi. Biochem. Biophys. Res. Commun. 334, 1198–1205.
[10] Marmagne, A. et al. (2004) Identification of new intrinsic proteins in *Arabidopsis* plasma membrane proteome. Mol. Cell Proteomics 3, 675–691.
[11] Hwang, H.H. and Gelvin, S.B. (2004) Plant proteins that interact with VirB2, the *Agrobacterium tumefaciens* pilin protein, mediate plant transformation. Plant Cell 16, 3148–3167.
[12] Thompson, J.D., Higgins, D.G. and Gibson, T.J. (1994) CLUSTAL W: improving the sensitivity of progressive multiple sequence alignment through sequence weighting, positions-specific gap penalties and weight matrix choice. Nucleic Acids Res. 22, 4673–4680.
[13] Kumar, S., Tamura, K. and Nei, M. (2004) MEGA3: Integrated software for molecular evolutionary genetics analysis and sequence alignment. Brief. Bioinform. 5, 150–163.
[14] Curtis, M. and Grossniklaus, U. (2003) A Gateway cloning vector set for high-throughput functional analysis of genes in planta. Plant Physiol. 133, 462–469.
[15] An, G., Costa, M.A., Mitra, A., Ha, S.-B. and Márton, L. (1988) Organ-specific and developmental regulation of the nopaline synthase promoter in transgenic tobacco plants. Plant Physiol. 88, 547–552.

[16] Clough, S.J. and Bent, A.F. (1998) Floral dip: a simplified method for *Agrobacterium*-mediated transformation of *Arabidopsis thaliana*. Plant J. 16, 735–743.
[17] Bauer, M., Dietrich, C., Nowak, K., Sierralta, W.D. and Papenbrock, J. (2004) Intracellular localization of *Arabidopsis* sulfurtransferases. Plant Physiol. 135, 916–926.
[18] Nilsson, T., Jackson, M. and Peterson, P.A. (1989) Short cytoplasmic sequences serve as retention signals for transmembrane proteins in the endoplasmic reticulum. Cell 58, 707–718.
[19] Contreras, I., Ortiz-Zapater, E. and Aniento, F. (2004) Sorting signals in the cytosolic tail of membrane proteins involved in the interaction with plant ARF1 and coatomer. Plant J. 38, 685–698.
[20] Rahier, A., Darnet, S., Bouvier, F., Camara, B. and Bard, M. (2006) Molecular and enzymatic characterizations of novel bifunctional 3beta-hydroxysteroid dehydrogenases/C-4 decarboxylases from *Arabidopsis thaliana*. J. Biol. Chem. 281, 27264–27277.
[21] Boevink, P., Santa Cruz, S., Hawes, C., Harris, N. and Oparka, K.J. (1996) Virus-mediated delivery of the green fluorescent protein to the endoplasmic reticulum of plant cells. Plant J. 10, 935–941.
[22] Boevink, P., Oparka, K., Santa Cruz, S., Martin, B., Betteridge, A. and Hawes, C. (1998) Stacks on tracks: the plant Golgi apparatus traffics on an actin/ER network. Plant J. 15, 441–447.
[23] Brandizzi, F., Snapp, E.L., Roberts, A.G., Lippincott-Schwartz, J. and Hawes, C. (2002) Membrane protein transport between the endoplasmic reticulum and the Golgi in tobacco leaves is energy dependent but cytoskeleton independent: evidence from selective photobleaching. Plant Cell 14, 1293–1309.
[24] Whatley, J.M., McLean, B. and Juniper, B.E. (1991) Continuity of chloroplast and endoplasmic reticulum membranes in *Phaseolus vulgaris*. New Phytol. 117, 209–218.
[25] Kaneko, Y. and Keegstra, K. (1996) Plastid biogenesis in embryonic pea leaf cells during early germination. Protoplasma 195, 59–67.
[26] Hanson, M.R. and Köhler, R.H. (2001) GFP imaging: methodology and application to investigate cellular compartmentation in plants. J. Exp. Bot. 52, 529–539.
[27] Andersson, M.X., Goksor, M. and Sandelius, A.S. (2007) Optical manipulation reveals strong attracting forces at membrane contact sites between endoplasmic reticulum and chloroplasts. J. Biol. Chem. 282, 1170–1174.
[28] Kelly, A.A. and Dörmann, P. (2004) Green light for galactolipid trafficking. Curr. Opin. Plant Biol. 7, 262–269.